

## Antiferromagnetic transitions in tetragonal-like BiFeO<sub>3</sub>

G. J. MacDougall,<sup>1</sup> H. M. Christen,<sup>2,\*</sup> W. Siemons,<sup>2</sup> M. D. Biegalski,<sup>3</sup> J. L. Zarestky,<sup>4,5</sup> S. Liang,<sup>2,6</sup>  
E. Dagotto,<sup>2,6</sup> and S. E. Nagler<sup>1,7</sup>

<sup>1</sup>Quantum Condensed Matter Division, Oak Ridge National Laboratory, Oak Ridge, Tennessee 37831, USA

<sup>2</sup>Materials Science and Technology Division, Oak Ridge National Laboratory, Oak Ridge, Tennessee 37831, USA

<sup>3</sup>Center for Nanophase Materials Sciences, Oak Ridge National Laboratory, Oak Ridge, Tennessee 37831, USA

<sup>4</sup>Department of Physics and Astronomy, Iowa State University, Ames, Iowa 50011, USA

<sup>5</sup>Division of Materials Science and Engineering, Ames Laboratory, Iowa State University, Ames, Iowa 50011, USA

<sup>6</sup>Department of Physics and Astronomy, University of Tennessee, Knoxville, Tennessee 37996, USA

<sup>7</sup>CIRE, University of Tennessee, Knoxville, Tennessee 37996, USA

(Received 14 July 2011; published 20 March 2012)

Recent studies have reported the existence of an epitaxially stabilized tetragonal-like (“*T*-like”) monoclinic phase in BiFeO<sub>3</sub> thin films with high levels of compressive strain. While their structural and ferroelectric properties are different from those of rhombohedral-like (“*R*-like”) films with lower levels of strain, little information exists on magnetic properties. Here, we report on a detailed neutron scattering study of a nearly phase-pure film of *T*-like BiFeO<sub>3</sub>. By tracking the temperature dependence and relative intensity of several superstructure peaks in the reciprocal lattice cell, we confirm antiferromagnetism with largely G-type character and  $T_N = 324$  K, significantly below a structural phase transition at 375 K, contrary to previous reports. Evidence for a second transition, possibly a minority magnetic phase with C-type character, is also reported with  $T_N = 260$  K. The coexistence of the two magnetic phases in *T*-like BiFeO<sub>3</sub> and the difference in ordering temperatures between *R*-like and *T*-like systems is explained through simple Fe-O-Fe bond distance considerations.

DOI: [10.1103/PhysRevB.85.100406](https://doi.org/10.1103/PhysRevB.85.100406)

PACS number(s): 77.55.Nv, 75.25.-j, 75.70.Ak, 77.80.bn

The oxide perovskite BiFeO<sub>3</sub> is the only known room temperature multiferroic,<sup>1</sup> with robust ferroelectricity below  $T_c = 1103$  K and long-wavelength cycloidal antiferromagnetism below  $T_N = 643$  K in bulk form.<sup>2</sup> A flurry of recent work indicates that thin films can exhibit large ferroelectric polarization,<sup>3,4</sup> novel magnetoelectric coupling effects,<sup>5</sup> and a series of strain-induced phase transitions with the promise of compelling device applications.<sup>6–11</sup> Currently there is particularly strong interest in the epitaxially stabilized tetragonal-like (“*T*-like”) monoclinic phase of BiFeO<sub>3</sub> induced by large compressive strains. This Rapid Communication presents experimental results on the nature of magnetism in essentially pure *T*-like films, and shows that the structural and antiferromagnetic phase transitions are distinct from one another, contrary to previous reports.<sup>12,13</sup>

Epitaxial strain is known to play a major role in determining properties of thin-film multiferroic materials.<sup>14–16</sup> In BiFeO<sub>3</sub>, even the slight compressive strain afforded by epitaxial growth on SrTiO<sub>3</sub> substrates changes the structure from bulk rhombohedral to “*R*-like” monoclinic with a  $\frac{c}{a}$  ratio near 1.03.<sup>3</sup> The large room temperature ferroelectric moment of bulk BiFeO<sub>3</sub> is retained, and with increasing strain the crucial out-of-plane ferroelectric moment is enhanced.<sup>4</sup> Antiferromagnetic order is largely G type<sup>17–19</sup> with a commensurability that depends on local structural considerations.<sup>19</sup>

When the compressive strain exceeds 4.5% a new phase appears with a  $\frac{c}{a}$  ratio near 1.25.<sup>6,7</sup> This “*T*-like” phase can be thought of as a monoclinic distortion from a predicted metastable  $P4mm$  tetragonal phase.<sup>20–22</sup> It is now understood to be part of a sequence of phases in BiFeO<sub>3</sub>: With compressive strain the structural progression is rhombohedral–(*R*-like) monoclinic–(*T*-like) monoclinic–tetragonal, similar to what is observed at morphotropic phase boundaries in lead-based

piezoelectric materials.<sup>11</sup> As has recently been pointed out by Damodaran *et al.*,<sup>23</sup> this response to strain is very different from that of a Poisson-like deformation. In a Poisson-like elastic regime, coherent strain between a film and substrate is only maintained up to a critical thickness.<sup>24</sup> BiFeO<sub>3</sub>, in contrast, responds via polymorphism similar to the epitaxial halides<sup>25</sup> or antimony, which can be epitaxially stabilized in the “gray tin” allotrope rather than the stable “white tin” phase in the bulk.<sup>26</sup>

While the ferroelectric transition temperature  $T_c$  of *R*-like films decreases with compressive strain,<sup>27</sup> its value is unknown for *T*-like BiFeO<sub>3</sub>. However, such films exhibit a structural phase transition between distinct *T*-like monoclinic phases at 375 K,<sup>12,28–30</sup> leading to the anticipation of strong coupling effects as the various transition temperatures become comparable.

Very little is known at this point about the magnetic properties of *T*-like phase of BiFeO<sub>3</sub>, in large part because magnetometry studies of antiferromagnetic films are often inconclusive due to the strong diamagnetic response of substrate materials. First-principles calculations for films with 6% compressive strain found near-degenerate energy scales for G-type and C-type magnetic structures, where adjacent antiferromagnetic layers are stacked with spins antiparallel and parallel, respectively.<sup>22</sup> Such calculations<sup>22,31</sup> predict that structures with a large  $\frac{c}{a}$  ratio, including the *T*-like phase, should exhibit ground states with C-type antiferromagnetic order.<sup>31</sup> In contrast, a room temperature neutron diffraction measurement on one phase-pure *T*-like BiFeO<sub>3</sub> film revealed a magnetic peak that is consistent with a G-type structure.<sup>6</sup> Subsequent Mössbauer measurements have recently been used to infer an antiferromagnetic transition at  $T_N = 360 \pm 20$  K,<sup>12</sup> within error equal to the above-mentioned structural transition.

This is remarkably lower than the transitions to G-type antiferromagnetism in *R*-like films that occurs with  $T_N$  near the bulk value of 643 K.<sup>19,27</sup>

In this communication, we report elastic neutron scattering measurements in epitaxially stabilized *T*-like BiFeO<sub>3</sub> on LaAlO<sub>3</sub> which go beyond previous studies in several important ways and provide important information about the nature of magnetism in this material. By measuring the temperature dependence of scattering at multiple half-integer Bragg positions, we confirm the existence of G-type antiferromagnetism implied by earlier measurements<sup>6</sup> and provide an estimate of the Néel temperature with neutrons:  $T_N = 324$  K. By additionally observing the  $T = 375$  K structural transition in the same experiment, our data clearly demonstrate that the two transitions are in fact decoupled. We further present evidence for a second magnetic phase showing C-type antiferromagnetism at a lower temperature, demonstrating macroscopic phase coexistence in a *T*-like BiFeO<sub>3</sub> film that does not contain the *R*-like polymorph. Through a comparison of scattering intensities at several magnetic Bragg peaks, it is inferred that spins in the G-type structure lie in the plane of the film. Aided by Monte Carlo calculations, we show that the essential difference in the magnetism of *R*-like and *T*-like films can be understood using straightforward considerations of Fe-O-Fe bond distances.

An epitaxial BiFeO<sub>3</sub> film of 300 nm thickness was grown on (001)-oriented LaAlO<sub>3</sub> substrates via pulsed laser deposition. (Pseudocubic notations are used throughout this communication.) Details about the growth technique and conditions are described elsewhere,<sup>11</sup> as are extensive x-ray scattering investigations of the quality and structural evolution of the film investigated here.<sup>28</sup>

The data in Ref. 28 (obtained on the same sample studied here) show that the film consists only of *T*-like BiFeO<sub>3</sub> ( $\frac{c}{a} = 1.23$ ), a small (<2%) amount of a polymorph that reversibly arises below the  $T = 375$  K transition due to tiling considerations, a negligible ( $\ll 0.1\%$ ) amount of polycrystalline bismuth oxide, and *no* measurable amount of the *R*-like phase. This near phase purity contrasts with some previous reports of BiFeO<sub>3</sub> films on LaAlO<sub>3</sub>, where a competing *R*-like phase occupies up to 30–60% of the sample volume.<sup>1,9</sup> Nonetheless, it is in agreement with numerous reports in the literature of up to 99% phase-pure *T*-like BiFeO<sub>3</sub> in samples of thickness 100 nm or greater.<sup>6,28,29</sup>

Neutron scattering measurements were performed using the HB1a Triple-Axis Spectrometer at the High-Flux Isotope Reactor in an elastic configuration with a fixed incident energy  $E_i = 14.7$  meV, pyrolytic graphite (PG) (002) monochromator and analyzer, instrument collimations 48'-48'-40'-60', and higher order contamination removed by standard PG filters. The film was aligned in the (H H L) scattering plane. For measurements at temperatures ranging from 10 K to 375 K, the sample was mounted in a closed cycle refrigerator (CCR) in a can with thermal contact assured by He exchange gas. Additional measurements from 40 K to 435 K were done using a high-temperature CCR which lacked exchange gas and from 300 K to 500 K using a furnace. Where presented below, data from the furnace were scaled to match the data from the CCR as laid out in the Supplemental Material.<sup>33</sup>

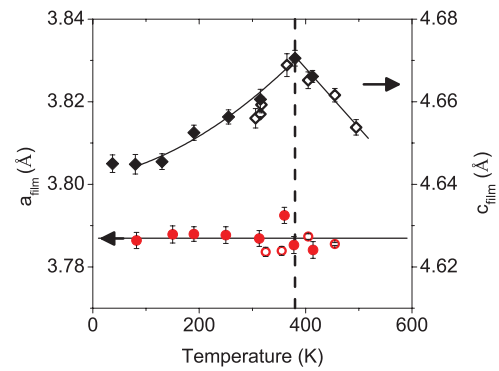


FIG. 1. (Color online) Temperature dependence of the out-of-plane (diamonds) and in-plane (circles) lattice parameters of the BiFeO<sub>3</sub> film. Closed symbols represent measurements taken with the high-temperature CCR apparatus upon warming from 40 K, and open symbols represent data taken with the furnace upon cooling from 500 K. A sharp change in the temperature dependence of  $c$  is seen at  $T^* \approx 375$  K (dashed line), without a concomitant change in  $a$ . This agrees with the *T*-like monoclinic to *T*-like monoclinic structural phase transition recently observed with x-ray scattering (Refs. 12,28–30). Solid lines are guides to the eye.

Neutron measurements confirmed that the BiFeO<sub>3</sub> film had a nearly tetragonal structure with the in-plane lattice constants epitaxially matched to the substrate. The room temperature lattice constants were  $a = 3.79$  Å,  $c = 4.66$  Å, consistent with the  $\frac{c}{a}$  ratio for the *T*-like phase reported by Christen *et al.*<sup>11</sup> and results from x-ray scattering on this sample.<sup>28</sup> Measurements of the film peak at (001) using both the high-temperature CCR and the furnace were used to track the evolution of the out-of-plane lattice parameter  $c$  with temperature. The results, shown in Fig. 1, reveal a significant evolution of  $c$  over the entire temperature range investigated, while the in-plane lattice parameter remained perfectly epitaxially matched to the substrate within resolution. A sharp cusp in the  $c$ -temperature curve at  $T^* \approx 380$  K reflects the existence of a structural phase transition between different *T*-like phases of BiFeO<sub>3</sub>, as reported in recent x-ray and Raman scattering studies.<sup>12,28–30</sup>

At low temperatures, neutron scattering showed superlattice peaks in the film at half-integer Bragg positions for the majority structural phase. The large  $\frac{c}{a}$  ratio of the *T*-like phase allows us to clearly distinguish between signal from it and one from, for example, a possible *R*-like impurity phase that might have escaped our attention in x-ray scattering measurements. Most of the observed peaks were characteristic of G-type order:  $(\frac{1}{2} \frac{1}{2} \frac{1}{2})$ ,  $(\frac{1}{2} \frac{1}{2} \frac{3}{2})$ ,  $(\frac{1}{2} \frac{1}{2} \frac{5}{2})$ ,  $(\frac{3}{2} \frac{3}{2} \frac{1}{2})$ , and  $(\frac{3}{2} \frac{3}{2} \frac{3}{2})$ . In addition, a peak was observed at the C-type wave vector  $(\frac{1}{2} \frac{1}{2} 0)$ . No significant signal was apparent at  $(00 \frac{1}{2})$  or  $(11 \frac{1}{2})$  positions, eliminating A-type antiferromagnetism. Figure 2 shows radial scans across four peaks at temperatures above (370 K) and below (37 K) the Néel temperatures determined below. All panels show a significant increase of scattering intensity at low temperature. The weak peaks remaining at 370 K in panels (a) and (c) might arise from residual magnetic short-range order or weak structural distortions. The temperature-independent background peaks in panels (b) and (c) are powder diffraction lines of unknown origin; it has been confirmed that the

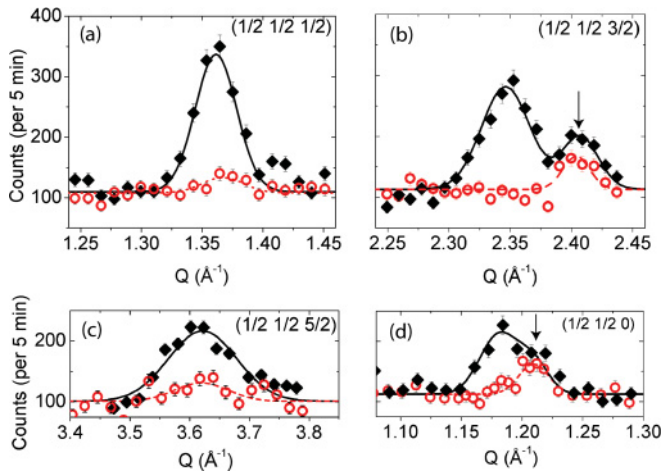


FIG. 2. (Color online) Elastic neutron scattering data at four half-integer film peaks at  $T = 370$  (open circles) and  $37$  K (closed diamonds) measured using the high-temperature CCR environment. Clear increased intensity at low  $T$  is seen at peaks associated with G-type antiferromagnetic order. Shown here are (a)  $(\frac{1}{2} \frac{1}{2} \frac{1}{2})$ , (b)  $(\frac{1}{2} \frac{1}{2} \frac{3}{2})$ , and (c)  $(\frac{1}{2} \frac{1}{2} \frac{5}{2})$ . Additional intensity at low  $T$  is also observed at (d)  $(\frac{1}{2} \frac{1}{2} 0)$ , which may indicate a small coexisting volume of C-type antiferromagnetism (see discussion in text). Arrows in (b) and (d) denote positions of temperature-independent background peaks. Solid lines are the results of fitting to simple Gaussians.

background peak in panel (d) is dependent on the choice of sample environment.

Temperature-dependent x-ray scattering confirmed that there is no structural transition in this sample between  $300$  K and  $375$  K.<sup>28</sup> The neutron data presented in Fig. 1 suggest no major modifications of the film structure over the entire temperature range investigated. At low temperatures, the observed intensity at  $(\frac{3}{2} \frac{3}{2} \frac{3}{2})$  is slightly less than 10% of that at  $(\frac{1}{2} \frac{1}{2} \frac{1}{2})$ , consistent with expectations based on the magnetic form factor of  $\text{Fe}^{3+}$ . Moreover, the intensity ratios of the half-integer peaks are inconsistent with any of the known common structural distortions observed in cubic perovskites. The limited data set available does not permit a complete refinement of the magnetic structure; however, the relative intensities of different  $(\frac{1}{2} \frac{1}{2} L)$  peaks imply that moments of the G-type structure are confined to the plane of the film. To within the resolution of the present measurements, no modulation of the G-type structure is visible. As mentioned above, the emergence of a peak at the  $(\frac{1}{2} \frac{1}{2} 0)$  Bragg position is at odds with a simple G-type picture. We further point out that the scattering at the  $(\frac{1}{2} \frac{1}{2} 0)$  position is much too intense to be associated with the minority structural phase identified by x-ray scattering, which would appear an order of magnitude weaker in neutron scattering experiments. Since only one peak has been detected, one cannot definitively rule out a structural phase transition, albeit with no visible effect in the lattice parameters in Fig. 1. More likely is the onset of a coexistence of two distinct magnetic ordering patterns at lower temperatures, both within the majority  $T$ -like structural phase. This latter possibility is consistent with the near degeneracy of G-type and C-type structures in the *ab initio* calculations.<sup>22</sup> A comparison of the relative intensities of  $(\frac{1}{2} \frac{1}{2} \frac{1}{2})$  and  $(\frac{1}{2} \frac{1}{2} 0)$

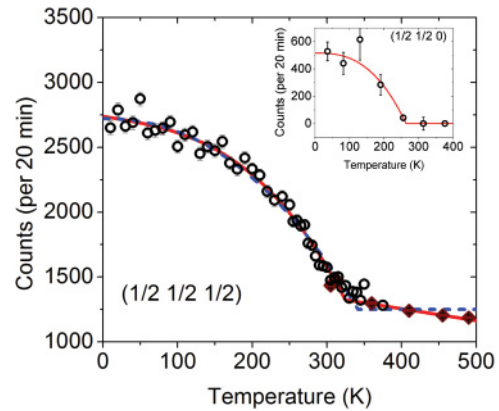


FIG. 3. (Color online) Plot of the neutron scattering intensity at the  $(\frac{1}{2} \frac{1}{2} \frac{1}{2})$  peak position as a function of temperature, measured with a furnace (closed diamonds) and a low-temperature CCR (open circles) upon cooling. The data from the furnace were adjusted by scaling using the ratio of measured Bragg peak heights and adjusting the background to match the range of data overlapped with the CCR. The solid (dashed) line is a fit assuming sloped (flat) background. Inset shows the evolution of the fitted  $(\frac{1}{2} \frac{1}{2} 0)$  peak height over background scaled to match counting time and conditions of main panel.

peaks suggests that 15–30% of the sample volume contains C-type antiferromagnetism in this scenario, depending on the orientation of the ordered spins. As the widths of the superlattice peaks measured in low-order Brillouin zones are comparable to the width of the substrate  $(2 \ 2 \ 0)$  peak, it is not possible in the present experiment to infer further information about the magnetic domain sizes or correlation lengths.

The magnetic transition temperature of the G-type order was determined from the measured intensity of the scattering at  $(\frac{1}{2} \frac{1}{2} \frac{1}{2})$ , as shown in the main panel of Fig. 3. Data from both the CCR and furnace were fit phenomenologically to a power-law temperature dependence in the range  $10 \text{ K} < T < T_N$ . Particular attention was also given to the fits of background above the magnetic transition, as a small amount of temperature dependence was observed up to  $500$  K, possibly associated with critical correlations above a continuous phase transition. Specifically, fits were performed with either linearly sloping or flat background. The former fit, shown as a solid line in Fig. 3, provides the superior description of the data and implies a transition temperature of  $T_N = 323 \pm 4$  K. We believe this to be the most reliable estimate of  $T_N$ ; however it should be noted that the fit with background held constant (dashed line in Fig. 3) yields  $T_N = 341 \pm 3$  K. The difference in these values reflects the magnitude of systematic error that might arise from different choices of background, and in fact these values may be taken as upper and lower bounds of reasonable estimates of  $T_N$ . For example, if a flat background is used and temperatures where the curve is concave-up are excluded, fits imply  $T_N = 327 \pm 5$  K. All values represent a significant decrease from the Néel temperatures reported for bulk  $\text{BiFeO}_3$  ( $643$  K)<sup>1</sup> and  $R$ -like films ( $600$ – $650$  K).<sup>27</sup> The magnetic transition is also clearly distinct from the structural transition identified in Fig. 1, in contrast to some previous reports.<sup>12,13</sup> The temperature dependence of the  $(\frac{1}{2} \frac{1}{2} 0)$  peak intensity, shown in the inset of Fig. 3, suggests that the C-type order is seen only at temperatures below  $T_{N,C} = 264 \pm 12$  K.



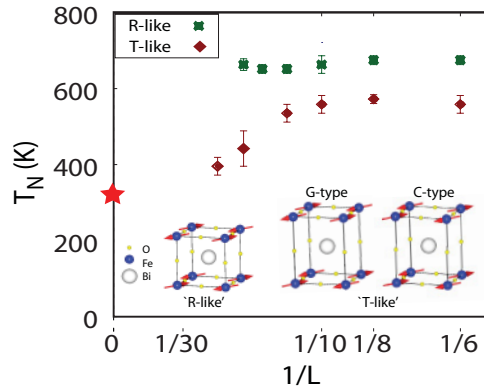


FIG. 4. (Color online) The convergence tendency of the ordering temperatures  $T_N$ , deduced from Monte Carlo calculations of staggered magnetization, susceptibility, and heat capacity in *R*-like and *T*-like  $\text{BiFeO}_3$  films. Details about the model used in the calculations are given in the main text. The star represents the value of  $T_N$  determined with neutrons. Also depicted are the magnetic ordering patterns observed in *R*-like and *T*-like  $\text{BiFeO}_3$ , with ordered moments chosen to lie in the *a-b* plane.

(Error bars are statistical and do not include possible sources of systematic errors.) No change is seen in the intensity of the  $(\frac{1}{2} \frac{1}{2} \frac{1}{2})$  scattering at  $T_{N,C}$ .

Simple considerations can provide insight into the different magnetic properties of the *R*-like and *T*-like phases of  $\text{BiFeO}_3$ . Transition-metal pseudopotential theory<sup>32</sup> predicts that the hopping matrix elements  $t_{pd}$  between the *d* orbitals of Fe and the *p* orbitals of O scale with the Fe-O interatomic distance  $r$  as  $1/r^{7/2}$ . Since perturbation theory near the atomic limit predicts that the Fe-Fe Heisenberg superexchange  $J$  depends on  $t_{pd}$  via  $J \propto t_{pd}^4$ , then overall  $J$  varies as  $J \propto r^{-14}$ . Using the known structures<sup>11</sup> and normalizing by the in-plane exchange constant of *R*-like  $\text{BiFeO}_3$ , this criterion implies that the *R*-like superexchange is characterized by the parameters  $J_x = J_y = 1.0$  and out-of-plane  $J_z = 0.87$ , while the *T*-like superexchange is characterized by  $J_x = 1.43$ ,  $J_y = 2.41$ , and  $J_z = 0.10$ . Although the precise results will be modified by additionally considering true bond angles, it is immediately apparent that the interactions in *T*-like  $\text{BiFeO}_3$  are expected to be much more two-dimensional than the interactions in the *R*-like material. Even though the in-plane values of exchange are higher for the *T*-like phase, our data imply that the net result is a suppression of magnetic order to much lower temperatures.

To explore this idea further, we have performed Monte Carlo simulations of the two cases utilizing an anisotropic

classical Heisenberg Hamiltonian with exchange couplings in the ratios discussed above. Calculations were carried out on a set of  $L \times L \times L$  sized tetragonal lattices, with transition temperatures determined by examining the staggered magnetization, susceptibility, and heat capacity. The precise magnitude of the superexchange was scaled to match the observed Néel temperature of the *R*-like  $\text{BiFeO}_3$  films, 643 K. Figure 4 plots the variation of  $T_N$  for the two cases with the Monte Carlo system size  $L$ . The convergence to the bulk limit is much slower for the *T*-like system, as expected because of its lower effective dimensionality. However, the present Monte Carlo results are sufficient to show that the ordering for the *T*-like phase will occur at a substantially lower temperature than for the *R*-like phase, in qualitative agreement with the experimental observations.

The weak interplanar coupling of *T*-like  $\text{BiFeO}_3$  also offers some insight into the possible coexistence of G-type and  $(\frac{1}{2} \frac{1}{2} 0)$  C-type antiferromagnetism at low temperatures. Both structures (illustrated in Fig. 4) are characterized by an antiferromagnetic arrangement of spins in the *a-b* plane, where the three-dimensional G-type structure is realized by antiferromagnetic stacking and C-type by ferromagnetic stacking along (00L). With very weak interplanar interactions, one can easily suppose that small differences in local structure or impurities can lead to either state, and this is consistent with the findings of *ab initio* calculations that the energy differences are very small and may in fact favor C-type order.

In summary, the results presented here shed light on the physics of the epitaxially stabilized *T*-like monoclinic phase of  $\text{BiFeO}_3$  which only exists in samples with high levels of compressive strain. Our film grown on  $\text{LaAlO}_3$  is nearly crystallographically phase pure, but gives evidence for phase coexistence of G-type and C-type antiferromagnetic order parameters. We estimate magnetic ordering temperature  $T_N = 323 \pm 4$  K for the G-type order, which is distinct from the structural phase transition seen at higher temperature and more than a factor of two lower than similar order seen in *R*-like films. We attribute this large reduction mainly to a reduced dimensionality associated with increased Fe-Fe distances in the out-of-plane direction.

Research supported by the US Department of Energy, Basic Energy Sciences. H.M.C., W.S., J.L.Z., E.D., and S.L. were supported by the Materials Science and Engineering Division, and G.J.M. and S.E.N. were supported by the Scientific User Facilities Division. Experiments were performed at the High Flux Isotope Reactor and the Center for Nanophase Materials Sciences, which are sponsored by the Scientific User Facilities Division.

\*christenhm@ornl.gov

<sup>1</sup>G. Catalan and J. F. Scott, *Adv. Mater.* **21**, 2463 (2009).

<sup>2</sup>See, e.g., M. Ramazanoglu, W. Ratcliff II, Y. J. Choi, Seongsu Lee, S.-W. Cheong, and V. Kiryukhin, *Phys. Rev. B* **83**, 174434 (2011).

<sup>3</sup>J. Wang *et al.*, *Science* **299**, 1719 (2003).

<sup>4</sup>H. W. Jang *et al.*, *Phys. Rev. Lett.* **101**, 107602 (2008).

<sup>5</sup>T. Zhao *et al.*, *Nature Mater.* **5**, 823 (2006).

<sup>6</sup>H. Béa *et al.*, *Phys. Rev. Lett.* **102**, 217603 (2009).

<sup>7</sup>R. J. Zeches *et al.*, *Science* **326**, 977 (2009).

<sup>8</sup>Z. Chen *et al.*, *Appl. Phys. Lett.* **96**, 252903 (2010).

<sup>9</sup>Z. H. Chen *et al.*, *Adv. Funct. Mater.* **21**, 133 (2011).

<sup>10</sup>D. Mazumdar *et al.*, *Nano Lett.* **10**, 2555 (2010).

- <sup>11</sup>H. M. Christen, J. H. Nam, H. S. Kim, A. J. Hatt, and N. A. Spaldin, *Phys. Rev. B* **83**, 144107 (2011).
- <sup>12</sup>I. C. Infante *et al.*, *Phys. Rev. Lett.* **107**, 237601 (2011).
- <sup>13</sup>K. T. Ko *et al.*, *Nature Comm.* **2**, 567 (2011).
- <sup>14</sup>J. H. Haeni *et al.*, *Nature (London)* **430**, 758 (2004).
- <sup>15</sup>K. J. Choi *et al.*, *Science* **306**, 1005 (2004).
- <sup>16</sup>D. G. Schlom, L.-Q. Chen, C.-B. Eom, K. M. Rabe, S. K. Streiffer, and J.-M. Triscone, *Annu. Rev. Mater. Res.* **37**, 589 (2007).
- <sup>17</sup>H. Béa, M. Bibes, S. Petit, J. Kreisel, and A. Barthélémy, *Phil. Mag. Lett.* **87**, 165 (2007).
- <sup>18</sup>X. Ke, P. P. Zhang, S. H. Baek, J. Zarestky, W. Tian, and C. B. Eom, *Phys. Rev. B* **82**, 134448 (2010).
- <sup>19</sup>W. Ratcliff II *et al.*, *Adv. Funct. Mater.* **21**, 1567 (2011).
- <sup>20</sup>C. Ederer and N. A. Spaldin, *Phys. Rev. Lett.* **95**, 257601 (2005).
- <sup>21</sup>D. Ricinchi, K. Y. Yun, and M. Okuyama, *J. Phys. Condens. Matter* **18**, L97 (2006).
- <sup>22</sup>A. J. Hatt, N. A. Spaldin, and C. Ederer, *Phys. Rev. B* **81**, 054109 (2010).
- <sup>23</sup>A. R. Damodaran, S. Lee, K. Jambunathan, S. MacClaren, and L. W. Martin, e-print [arXiv:1110.3847v1](https://arxiv.org/abs/1110.3847v1).
- <sup>24</sup>J. W. Matthews and A. E. Blakeslee, *J. Cryst. Growth* **27**, 118 (1974).
- <sup>25</sup>R. F. C. Farrow *et al.*, *J. Vac. Sci. Tech. B* **1**, 222 (1983).
- <sup>26</sup>R. F. C. Farrow *et al.*, *J. Cryst. Growth* **54**, 507 (1981).
- <sup>27</sup>I. C. Infante *et al.*, *Phys. Rev. Lett.* **105**, 057601 (2010).
- <sup>28</sup>W. Siemons, M. D. Biegalski, J. H. Nam, and H. M. Christen, *Appl. Phys. Express* **4**, 095801 (2011).
- <sup>29</sup>J. Kreisel *et al.*, *J. Phys. Condens. Matter* **23**, 342202 (2011).
- <sup>30</sup>H.-J. Liu *et al.*, *Phys. Rev. B* **85**, 014104 (2012).
- <sup>31</sup>O. Dieguez, O. E. Gonzalez-Vazquez, J. C. Wojdel, and J. Iniguez, *Phys. Rev. B* **83**, 094105 (2011).
- <sup>32</sup>W. A. Harrison, *Electronic Structure and the Properties of Solids* (Dover, New York, 1989), Chap. 19.
- <sup>33</sup>See Supplemental Material at <http://link.aps.org/supplemental/10.1103/PhysRevB.85.100406> for a description of the procedure.